Fractional Calculus in the Transient Analysis of Viscoelastically Damped Structures

Ronald L. Bagley* and Peter J. Torvik†
Air Force Institute of Technology, Wright-Patterson Air Force Base, Ohio

Fractional calculus is used to model the viscoelastic behavior of a damping layer in a simply supported beam. The beam is analyzed by using both a continuum formulation and a finite element formulation to predict the transient response to a step loading. The construction of the finite element equations of motion and the resulting nontraditional orthogonality conditions for the damped mode shapes are presented. Also presented are the modified forms of matrix iteration required to calculate eigenvalues and mode shapes for the damped structure. The continuum formulation, also incorporating the fractional calculus model, is used to verify the finite element approach. The location of the poles (damping and frequency) are found to be in satisfactory agreement, as are the modal amplitudes for the first several modes.

Nomenclature

$\{\ \}$	= column matrix
$\{\ \}^T$	= row matrix
$[\ ]$	= square matrix
$a_n(t)$	= modal participation function
$A_n(s)$	= Laplace transform of modal participation function
G_0, G_1	= model parameters
$\{F(s)\}$	= Laplace transform of applied forces
$[K]$	= stiffness matrix
$[M]$	= mass matrix
t	= time
$\{x(t)\}$	= nodal displacements
$\{X(s)\}$	= Laplace transform of nodal displacements
α	= model parameter
$\gamma(t)$	= shear strain history
$\gamma^*(s), \gamma^*(\omega)$	= Laplace and Fourier transforms of the strain history
λ_n	= nth eigenvalue
$\tau(t)$	= shear stress history
$\tau^*(s), \tau^*(\omega)$	= Laplace and Fourier transform of the stress history
$\{\phi_n\}$	= nth mode shape
$(\bar{\ })$	= expanded equations of motion
$(\hat{\ })$	= quasimodes and quasieigenvalues used in the iterations for higher modes

Introduction

THE fractional calculus approach to the analysis of viscoelastically damped structures has several very attractive features. The first is that the mathematical form of the fractional calculus viscoelastic model has its foundation in accepted molecular theories governing the mechanical behavior of viscoelastic media.[1] The model satisfies the Second Law of Thermodynamics[2] and predicts elliptic stress-strain hysteresis loops for viscoelastic materials.[3] This viscoelastic model has very few parameters, thereby lending itself to straightforward and accurate least-squares fits to measured frequency-dependent mechanical properties. To date, more than 130 viscoelastic materials have been described in this way, producing models accurate over at least three, and typically six, decades of frequency.[4-6] When introduced into finite element equations of motion, the fractional calculus models produce well-posed differential equations of motion possessing closed form solutions.[7] Structural responses can be calculated for any loading history having a Laplace transform, and the responses are always real, continuous, and causal functions of time.[2] All these features of the fractional calculus approach make it an attractive alternative to existing methods.

At present, the viscoelastic models popularly applied in structural analysis employ one of three approaches. The first is to relate time-dependent stresses to time-dependent strains through a series of time derivatives acting on the stress and strain fields. This is, of course, the classical viscoelastic model presented in many textbooks. The major drawback of this approach is that a large number of derivative terms, acting on stress and strain, are required to model the frequency-dependent stiffness and damping properties for many viscoelastic materials.[8] This complicates the process of performing a least-squares fit of the model to the data. Once the model has been developed, the equations of motion (which have been made extremely complex through the inclusion of many derivative terms) remain to be solved.

An alternative approach to modeling viscoelastic behavior is to store the value of the complex frequency-dependent modulus at many frequencies in the computer and retrieve the data as necessary to calculate the response. Experimental error in the data may lead to a stored modulus that does not satisfy the special mathematical relationships that must exist between the real and imaginary parts of a transform.[9] Another drawback of this approach is the computer memory and time required to calculate any nonperiodic response of the structure. A completely numerical evaluation of the inverse Laplace or Fourier transform must be used to calculate the response at each point in time for which the solution is desired.

Because these two techniques are only marginally attractive, the "structural damping model" is commonly used to model viscoelastic behavior. The attractive feature of this model is its simplicity. One models the modulus with a complex constant chosen to approximate the modulus over the entire frequency range of interest. It is easy to show that this model can lead to violations of the Second Law of Thermodynamics, as solutions to the resulting equations of motion may predict an exponentially growing response to decreasing loads. This may be avoided by using a function that changes the sign on the imaginary part of the modulus for negative frequencies; but the modified model then predicts a noncausal structural response

Presented as Paper 83-0901 at the AIAA/ASME/ASCE/AHS 24th Structures, Structural Dynamics and Materials Conference, Lake Tahoe, Nev., May 2-4, 1983; received June 16, 1983; revision received Sept. 5, 1984. This paper is declared a work of the U.S. Government and therefore is in the public domain.

*4950 Test Wing; formerly, Associate Professor, Department of Engineering Mechanics, U.S. Air Force Academy.

†Professor and Head, Department of Aeronautics and Astronautics.

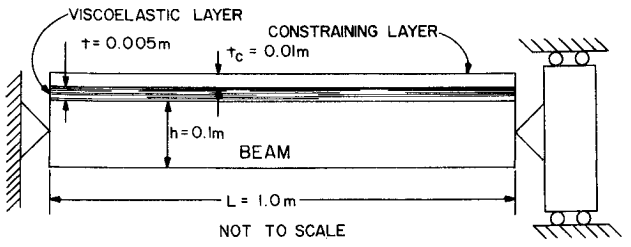

Fig. 1 Simply supported cantilever beam.

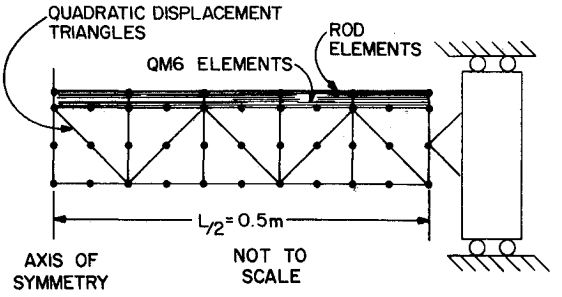

Fig. 2 Finite element grid for beam.

to impulsive loading, as was shown by Crandall.[10] As the noncausal behavior is small for lightly damped structures, one may be tempted to use this model to calculate the transient response in such cases. At larger levels of damping, however, the noncausal behavior (the amount of response before the load is applied) becomes more appreciable and the credibility of this model comes into serious question. Although not truly appropriate for transient motion, this model describes sinusoidal, steady-state motion of the structure very well.

These three means of including viscoelasticity or structural damping into analyses all have disadvantages. In contrast, the fractional calculus model is an attractive alternative in that it produces a compact analytic representation of a complex modulus, well behaved in both the frequency and time domains, and predicts causal structural responses.

The fractional calculus appraoch to modeling viscoelastic behavior began with Nutting's observation that stress-relaxation phenomena could be modeled by fractional powers of time[11] instead of decaying exponentials. Scott-Blair's work[12] suggested the first use of time derivatives of fractional order to model Nutting's observations. Caputo[13] independently suggested the use of fractional calculus to model the viscoelastic behavior of geological strata. Several other authors—i.e., Slonimsky,[14] Smit and deVries,[15] and Calleja and Guzman[16]—have suggested very similar fractional calculus models for the viscoelastic phenomenon. Shestopal[17] has discussed mechanisms whereby tungsten and platinum at high temperatures behave as a generalized Maxwell body with exponents of ⅓ or ½, and related these to the work of Shermergor,[18] who observed that such models are equivalent to fractional differentiation. While first explored as an empirical method of describing viscoelastic behavior, the fractional calculus approach has recently been linked with established molecular theories governing the behavior of viscoelastic media.[1] This link removes fractional calculus models from the realm of empirical "curve fits" and enables the models to be used in structural analysis with much greater confidence.

Although the ability of the fractional calculus model to predict the transient response of a single-degree-of-freedom system has previously been established through comparison with experiment,[19] it is the purpose of this paper to demonstrate the application of the fractional calculus model to the finite element analysis of a multi-degree-of-freedom structure of engineering interest. The problem chosen is the transient response of a simply supported beam with a constrained viscoelastic damping layer (Fig. 1). We feel that the results of the analyses that follow demonstrate that the fractional calculus approach contributes substantially to the analysis of transient motion in viscoelastically damped structures.

The Problem

We wish to demonstrate the methods used in calculating the transient response of a moderately damped structure based on a finite element formulation of the equations of motion, incorporating a fractional calculus model of the damping material. In particular, we will describe the construction of the equations of motion, the resulting nontraditional orthogonality conditions for the damped mode shapes, and the modified form of matrix iteration used to find mode shapes and eigenvalues. Finally, we will calculate the transient response of the beam.

The results of the finite element solution will be compared with the predictions of the sixth-order continuum beam theory for constrained layer damping. These results will be obtained by using the correspondence principle to introduce the fractional calculus model of the constraining layer into the equation of motion and boundary conditions. Since the damped mode shapes are sinusoidal in the simply supported case, the continuum model can be solved for transient response in a relatively straightforward manner. Consequently, we will be comparing a continuum formulation and a finite element formulation, both employing the same fractional calculus model of the damping layer.

We believe the simply supported constrained layer beam to be a good test case. The presence of the constraining layer increases the effective damping of the viscoelastic layer, insuring a moderately damped structure. The structure and the loading are symmetric, requiring us to perform the finite element analysis on only half of the beam (Fig. 2). This reduces the required number of degrees of freedom by almost half. The particular loading case we will consider is a unit step load, applied downward at midspan. Before proceeding to the analyses, we will review certain aspects of the use of fractional calculus in viscoelastic models.

The Fractional Calculus Viscoelastic Model

The form of the model considered here is based on its ability to portray accurately the mechanical properties of many materials in the rubbery and transition regions of the material. For such cases, let

$$\tau(t) = G_0\gamma(t) + G_1 D^\alpha[\gamma(t)] \tag{1}$$

The general form of this model is identical, or almost identical, to all of the fractional calculus relationships reported in the literature referenced above. The time-dependent shear stress $\tau(t)$ is expressed as a superposition of an elastic term $G_0\gamma(t)$ and a viscoelastic term containing a derivative of fractional order, α. The fractional derivative

$$D^\alpha[x(t)] = \frac{1}{\Gamma(1-\alpha)}\frac{\mathrm{d}}{\mathrm{d}t}\int_0^t \frac{x(\tau)}{(t-\tau)^\alpha}\,\mathrm{d}\tau \qquad 0<\alpha<1 \tag{2}$$

as used here is the inverse operation of fractional integration attributed to Riemann and Liouville.[20]

To demonstrate the manner in which this model characterizes the frequency-dependent properties of the materials, the Fourier transform is used

$$F[x(t)] = \int_{-\infty}^{\infty} x(t)e^{-i\omega t}\mathrm{d}t = x^*(\omega) \tag{3}$$

Since we will be dealing with those functions, $x(t)$, which are zero for negative time, the lower limit of integration may be

set at zero. Taking the transform of the fractional derivative, as defined above, produces a useful relationship.

$$F[D^{\alpha}[x(t)]] = (i\omega)^{\alpha}F[x(t)] \tag{4}$$

A similar relationship holds for Laplace transforms.

$$L[D^{\alpha}[x(t)]] = s^{\alpha}L[x(t)] \tag{5}$$

where

$$L[x(t)] = \int_0^{\infty} x(t)e^{-st}dt \tag{6}$$

The Fourier transform of the fractional derivative model, Eq. (1), is then

$$\tau^*(\omega) = G_0\gamma^*(\omega) + G_1(i\omega)^{\alpha}\gamma^*(\omega) \tag{7}$$

where $\tau^*(\omega)$ and $\gamma^*(\omega)$ are the transforms of the stress and strain histories and G_0, G_1, and α the parameters of the model. Thus, the fractional derivative model predicts a frequency-dependent complex modulus of the form

$$G^*(\omega) = G_0 + G_1\cos(\pi\alpha/2)\omega^{\alpha} + iG_1\sin(\pi\alpha/2)\omega^{\alpha} \tag{8}$$

The properties of Butyl B252 will be used in this example. The static modulus G_0 is[21]

$$G_0 = 7.6\times 10^5 \text{ N/m}^2 \tag{9}$$

The order of the fractional derivative α is taken to be one half,

$$\alpha = 0.5 \tag{10}$$

and the coefficient G_1 is determined by performing a least-squares fit to the measured complex modulus[22] as shown in Fig. 3. Notice the excellent agreement between the model and the measured data points.

$$\tau(t) = (7.6\times 10^5)\gamma(t) + (2.95\times 10^5)D^{1/2}[\gamma(t)] \tag{11}$$

for t in seconds and τ in Newtons/meter^2.

The agreement between the model and the data is no accident. The mathematical form of the model, Eq. (11), is also motivated by molecular theory governing the behavior of viscoelastic media. The molecular theory of Rouse[23] for the mechanical properties of dilute polymer solutions, modified by Ferry et al.[24] for application to polymer solids with no cross-linking, predicts a constitutive relationship of the form[1]

$$\tau(t) = (3\mu\rho RT/2M)^{1/2}D^{1/2}[\gamma(t)] \tag{12}$$

Here, μ is the steady flow viscosity, ρ the density, R the universal gas constant, T the absolute temperature, and M the molecular weight. The appearance of the one-half derivative is striking. Equation (12) contains no elastic term because the molecular theory does not consider cross-linking; hence, it is a complete description only for a material that cannot sustain a static load.

Although the model of Butyl B252 shown in Fig. 3 and in Eq. (11) is an empirical curve-fit, the presence of the one-half derivative both in the fit and in Eq. (12) enables one to use the model with greater confidence. The model for Butyl B252 is valid from zero frequency (static loading) through 10^4 cycles/s. This is precisely the frequency range in which we wish to calculate the transient response of the beam. Consequently, a fractional derivative of one-half will be used in the analysis to follow. The literature cited above provides both empirical and theoretical bases for this. There are, however, materials for which one-half is not the best choice. The analyses to follow may be accomplished for α taking the value

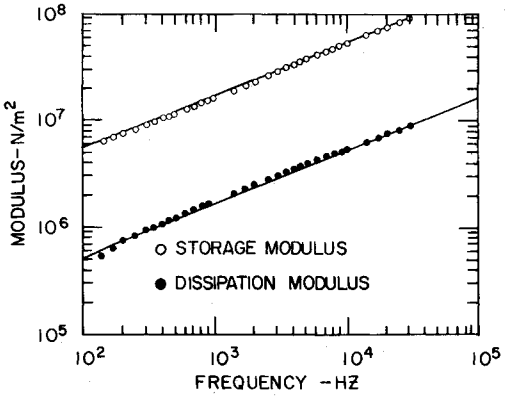

Fig. 3 Fractional calculus model for Butyl B252 (dissipation modulus plotted down one decade).

of any rational fraction between 0 and 1, but the number of calculations required varies proportionally with the magnitude of the denominator of α.

The Continuum Formulation

We wish to determine the transient response of a simply supported beam with a constrained layer-damping application (Fig. 1) by using modal analysis. We begin with the sixth-order differential equation of motion for the damped beam,[25]

$$\frac{\partial^6 w}{\partial x^6} - g(1+Y)\frac{\partial^4 w}{\partial x^4} + \frac{(ph)_e}{D_t}\left(\frac{\partial^4 w}{\partial x^2\partial t^2} - g\frac{\partial^2 w}{\partial t^2}\right) = \frac{1}{D_t}\left(\frac{\partial^2 q}{\partial x^2} - gq\right) \tag{13}$$

The constant coefficients in this equation are defined by

$$D_t = \frac{E_b h^3}{12} + \frac{E_c t_c^3}{12} \tag{14}$$

$$g = \frac{G^*}{t_v}\left(\frac{1}{E_b h} + \frac{1}{E_c t_c}\right) \tag{15}$$

$$d = \left(t_v + \frac{h+t_c}{2}\right) \tag{16}$$

$$Y = \frac{d^2}{D_t}\left(\frac{1}{E_b h} + \frac{1}{E_c t_c}\right)^{-1} \tag{17}$$

where E_b and E_c are the elastic moduli of the beam and the constraining layer; h and t_c the depths of the beam and the constraining layer; t_v and G^* the depth and shear modulus of the damping layer; $(ph)_e$ the mass per unit length of the composite beam; and q the distributed vertical load on the beam. This configuration has been discussed more completely elsewhere.[26,27]

The boundary conditions associated with the simply supported case are zero displacements at both ends,

$$w(x,t) = 0; \qquad x = 0, L \tag{18}$$

zero bending moments at both ends,

$$\frac{\partial^2 w}{\partial x^2} = 0; \qquad x = 0, L \tag{19}$$

and zero axial loads in the constraining layer and the beam at the ends.

This condition is satisfied if

$$\frac{\partial^4 w}{\partial x^4} - gY\frac{\partial^2 w}{\partial x^2} + \frac{(ph)_e}{D_t}\frac{\partial^2 w}{\partial t^2} = 0; \qquad x = 0, L \tag{20}$$

For the simply supported beam, an assumed solution of the form

$$w(x,t) = \sin(n\pi x/L)a_n(t), \qquad n = 1,2,3... \tag{21}$$

satisfies all boundary conditions. Substituting this assumed solution into the equation of motion and performing the Laplace transform produces an auxiliary equation of the form

$$-\left(\frac{n\pi}{L}\right)^6 - g(1+Y)\left(\frac{n\pi}{L}\right)^4 - \frac{(ph)_e}{D_t}\left[\left(\frac{n\pi}{L}\right)^2 + g\right]s^2 = 0 \tag{22}$$

The frequency-dependent modulus resulting from the fractional calculus is introduced into the auxiliary equation by invoking the correspondence principle.[28] Taking the Laplace transform of Eq. (1) and noting the relationship in Eq. (5), the transform of the viscoelastic stress-strain law is

$$\tau^*(s) = G_0\gamma^*(s) + G_1 s^\alpha \gamma^*(s) \tag{23}$$

Thus, the appropriate shear modulus to use in the correspondence principle is

$$G^*(s) = G_0 + G_1 s^\alpha \tag{24}$$

For $\alpha = \frac{1}{2}$, Eq. (22) produces

$$D(s) = -\left(\frac{n\pi}{L}\right)^6 - (g_0 + g_1 s^{1/2})(1+Y)\left(\frac{n\pi}{L}\right)^4 - \frac{(ph)_e}{D_t}\left[\left(\frac{n\pi}{L}\right)^2 s^2 + g_0 s^2 + g_1 s^{5/2}\right] \tag{25}$$

where the roots satisfy $D(s_j) = 0$ and

$$g_0 = \frac{G_0}{t_v}\left(\frac{1}{E_b h} + \frac{1}{E_c t_c}\right) \tag{26}$$

and

$$g_1 = \frac{G_1}{t_v}\left(\frac{1}{E_b h} + \frac{1}{E_c t_c}\right) \tag{27}$$

This is a fifth-order polynomial in $s^{1/2}$ which, at its roots, takes the form

$$D(s_j) = (s^{1/2} - s_1)(s^{1/2} - s_2)(s^{1/2} - s_3)(s^{1/2} - s_4)(s^{1/2} - s_5) = 0 \tag{28}$$

Since the coefficients in Eq. (25) are real, roots s_1-s_5 occur in complex conjugate pairs or are real. In this case, we find two sets of conjugate pairs and one real root.

To solve for the transient response to a unit step load applied at the midspan of the beam at time zero, the load is represented as

$$q(x,t) = \delta(x - L/2)u_0(t) \tag{29}$$

where δ denotes a spatial delta function.

Having obtained the roots of the auxiliary equation, one can return to the forced equation of motion [Eq. (13)] and determine the Laplace transform of the contribution of each mode to the transient response. To find the contribution of the nth mode to the response, assume $w(x,t)$ to be as given in Eq. (21), substitute this form into Eq. (13), multiply both sides by $\sin n\pi x/L$, integrate from 0 to L, and take the Laplace transform of the resulting fractional order differential equation. The equation for the nth mode is

$$A_n(s) = \frac{-2}{LD_t}\left[\left(\frac{n\pi}{L}\right)^2 + (g_0 + g_1 s^{1/2})\right]\frac{1}{sD(s)}\left(\sin\frac{n\pi}{2}\right) \tag{30}$$

where $D(s)$ is defined by Eq. (25). Thus, we can construct the Laplace transform of the transient response of the damped beam using the continuum formulation.

The Finite Element Formulation

The finite element formulation of the equations of motion for the damped beam begins in the traditional fashion, except for the treatment of those elements in the viscoelastic layer (Fig. 2). The stiffness matrices for the rectangular elements used in the viscoelastic layer are first constructed as though the elements were elastic. The elastic shear modulus is then factored out of each term in the element stiffness matrix,

$$[K_e] = \frac{E}{2(1+\nu)}[K'] \tag{31}$$

and the elastic-viscoelastic correspondence principle[28] is again applied. Replacing the elastic shear modulus with the representation obtained from the fractional calculus viscoelastic model, Eq. (24), produces

$$[K_e(s)] = (G_0 + G_1 s^\alpha)[K'] \tag{32}$$

With $\alpha = \frac{1}{2}$ the general form of the finite element equations of motion in the transform domain becomes

$$[s^2[M] + (G_0 + G_1 s^{1/2})[K'] + [K]]\{X(s)\} = \{F(s)\} \tag{33}$$

where $[M]$ is the mass matrix containing terms from the elastic and viscoelastic finite elements in the beam, $[K']$ the stiffness matrix constructed from the finite elements in the viscoelastic layer with the shear modulus factored out, and $[K]$ the normal stiffness matrix for the elastic beam and the elastic constraining layer.

As shown in Fig. 2, the elastic constraining layer is modeled by four-degree-of-freedom (DOF) rod elements and consistent mass matrices. The elastic beam is modeled using quadratic displacement triangles and their consistent mass matrices. The viscoelastic layer is modeled by eight DOF rectangular QM6 elements[29] and diagonal lumped mass matrices, where a quarter of the element mass is associated with each DOF.

Putting the equations of motion in more compact form yields

$$[s^2[M] + s^{1/2}[K_1] + [K_0]]\{X(s)\} = \{F(s)\} \tag{34}$$

where

$$[K_0] = G_0[K'] + [K] \tag{35}$$

and

$$[K_1] = G_1[K'] \tag{36}$$

We now wish to decouple the equations of motion and solve for the modal contributions to the transient response of the beam. Consequently, we must solve the homogeneous equations for eigenvectors and eigenvalues and construct an orthogonal transformation to decouple the forced equations of motion. However, it is impossible to construct an orthogonal transformation that decouples, in general, the equations of motion in their present form [Eq. (34)]. The problem is that traditional methods cannot be applied because elements in the stiffness matrix contain the Laplace parameter. One approach might be to construct an orthogonal transformation that simultaneously diagonalizes the three real, symmetric matrices, $[M]$, $[K_1]$, and $[K_0]$. Unfortunately, this approach will not work for most situations.

An approach that does work is to pose the equations of motion in terms of two real, square, symmetric matrices. This revised form of the equation of motion is

$$s^{1/2}\begin{bmatrix} 0 & 0 & 0 & M \\ 0 & 0 & M & 0 \\ 0 & M & 0 & 0 \\ M & 0 & 0 & K_1 \end{bmatrix}\begin{Bmatrix} \{X(s)\}\ s^{3/2} \\ \{X(s)\}\ s \\ \{X(s)\}\ s^{1/2} \\ \{X(s)\} \end{Bmatrix} + \begin{bmatrix} 0 & 0 & -M & 0 \\ 0 & -M & 0 & 0 \\ -M & 0 & 0 & 0 \\ 0 & 0 & 0 & K_0 \end{bmatrix}\begin{Bmatrix} \{X(s)\}\ s^{3/2} \\ \{X(s)\}\ s \\ \{X(s)\}\ s^{1/2} \\ \{X(s)\} \end{Bmatrix} = \begin{Bmatrix} 0 \\ 0 \\ 0 \\ \{F(s)\} \end{Bmatrix} \tag{37}$$

and will be referred to as the expanded equations of motion. Notice that the lowest set of partitioned matrix equations is the original equation of motion and that all of the other sets are satisfied identically. The importance of the expanded set of equations is that they lead us to orthogonality conditions for the mode shapes of the damped beam, $\{\phi_j\}$.

The mode shapes must satisfy the following equations:

$$\lambda_j\begin{bmatrix} 0 & 0 & 0 & M \\ 0 & 0 & M & 0 \\ 0 & M & 0 & 0 \\ M & 0 & 0 & K_1 \end{bmatrix}\begin{Bmatrix} \lambda_j^3\{\phi_j\} \\ \lambda_j^2\{\phi_j\} \\ \lambda_j\{\phi_j\} \\ \{\phi_j\} \end{Bmatrix} + \begin{bmatrix} 0 & 0 & -M & 0 \\ 0 & -M & 0 & 0 \\ -M & 0 & 0 & 0 \\ 0 & 0 & 0 & K_0 \end{bmatrix}\begin{Bmatrix} \lambda_j^3\{\phi_j\} \\ \lambda_j^2\{\phi_j\} \\ \lambda_j\{\phi_j\} \\ \{\phi_j\} \end{Bmatrix} = \begin{Bmatrix} 0 \\ 0 \\ 0 \\ 0 \end{Bmatrix} \tag{38}$$

Expressed in more compact notation, this becomes

$$\lambda_j[\tilde{M}]\{\tilde{\phi}_j\} + [\tilde{K}]\{\tilde{\phi}_j\} = \{0\} \tag{39}$$

where $[\tilde{M}]$ and $[\tilde{K}]$ are pseudo-mass and -stiffness matrices, respectively, and $\{\tilde{\phi}_j\}$ is a pseudo-eigenvector. The orthogonality conditions for the eigenvalue problem posed in Eq. (39) are

$$\{\tilde{\phi}_r\}^T[\tilde{M}]\{\tilde{\phi}_j\} = 0 \qquad \lambda_r \neq \lambda_j \tag{40}$$

and

$$\{\tilde{\phi}_r\}^T[\tilde{K}]\{\tilde{\phi}_j\} = 0 \qquad \lambda_r \neq \lambda_j \tag{41}$$

For $\lambda_r = \lambda_j$, the multiplications produce the elements of diagonal matrices $[\tilde{m}_r]$ and $[\tilde{k}_r]$. Posing Eq. (40) in terms of the actual mode shapes of the damped structure, $\{\phi_r\}$ and $\{\phi_j\}$ (instead of the expanded eigenvectors $\{\tilde{\phi}_r\}$ and $\{\tilde{\phi}_j\}$), produces

$$(\lambda_j^3 + \lambda_j^2\lambda_r + \lambda_j\lambda_r^2 + \lambda_r^3)\{\phi_r\}^T[M]\{\phi_j\} + \{\phi_r\}^T[K_1]\{\phi_j\} = 0 \qquad \lambda_r \neq \lambda_j \tag{42}$$

Similarly, the orthogonality condition for the pseudo-stiffness matrix [Eq. (41)] expressed in terms of the mode shapes $\{\phi_r\}$ and $\{\phi_j\}$ is

$$-(\lambda_j^3\lambda_r + \lambda_j^2\lambda_r^2 + \lambda_j\lambda_r^3)\{\phi_r\}^T[M]\{\phi_j\} + \{\phi_r\}^T[K_0]\{\phi_j\} = 0 \qquad \lambda_r \neq \lambda_j \tag{43}$$

Note that if the viscoelastic damping matrix $[K_1] = 0$ then Eqs. (42) and (43) would reduce to the traditional orthogonality conditions with respect to the mass and stiffness matrices for an undamped structure.

A potential obstacle to the numerical analysis is that the pseudo-mass and pseudo-stiffness matrices appearing in Eqs. (37) and (38) are of order four times greater than the number of degrees of freedom in the structure. Another potential problem concerns the magnitudes of the eigenvalues λ. Although not readily apparent, the eigenvalues occur in groups of four (two pairs of complex conjugates) where, for small damping, all four eigenvalues have approximately the same magnitudes. Hence, classical methods of matrix iteration will have considerable difficulty separating eigenvalues and eigenvectors. These problems can be overcome by modifying the process of matrix iteration.

We begin by returning to the bottom set of partitioned matrix equations appearing in Eq. (38),

$$[\lambda_j^4[M] + \lambda_j[K_1] + [K_0]]\{\phi_j\} = \{0\} \tag{44}$$

and using this equation to construct a recursive relationship to find the first mode shape and associated eigenvalue.

$$[\lambda_1^{(\ell)}[K_1] + [K_0]]^{-1}[M]\{\phi_1\}^{(\ell+1)} = -\frac{1}{\lambda_1^{4(\ell+1)}}\{\phi_1\}^{(\ell+1)} \tag{45}$$

Here, ℓ and $\ell+1$ denote successive estimates of the first eigenvalue and first mode shape. This recursive relationship differs from the classical approach by using successive applications of the matrix iteration processes. Initial estimates of the first eigenvalue, $\lambda_1^{(1)}$, and the first mode, $\{\phi_1\}^{(1)}$, are made and substituted into the recursive relationship. Matrix iteration is then applied [with the eigenvalue on the left-hand side of Eq. (45) held fixed] until the mode shape stops changing. This produces second estimates of the mode shape and eigenvalue. These estimates are substituted into the recursive relationship and matrix iteration is again applied (with $\lambda_1^{(2)}$ held fixed on the left-hand side) until the mode shape stops changing. This produces the third estimates of the mode shapes and eigenvalue. This process is continued until successive estimates of the eigenvalue converge. Actually, it must be done four times. Since each estimate is of the fourth power of $\lambda_1^{(\ell+1)}$, each of the four branches of the fourth power must be used on the left-hand side. Thus the recursive process produces four distinct values of λ_1, each corresponding to a different branch of the quarter-root function. All, however, are associated with the lowest frequency of the structure.

The four eigenvalues occur in complex conjugate pairs, each pair describing a different motion of the structure. One pair forms poles in the system transfer function and produces exponentially decaying sinusoidal motion. The other pair forms poles in the system transfer function on other Riemann surfaces and produces a monotonically decreasing response of the structure. The decaying sinusoidal motion describes motion at the natural frequencies of the system, while the monotonically decreasing motion describes a creep response that may occur.

Having obtained the smallest eigenvalues and associated mode shapes for the structure, we must now calculate the eigenvalues and mode shapes associated with the higher natural frequencies. The recursive relationships used to obtain those eigenvalues and mode shapes associated with the second resonance follow from adapting Turner's method to this problem.[30]

$$\left[\lambda_2^{(\ell)}[K_1] + [K_0]\right]^{-1}[M]\{\hat{\phi}_1\} = -(1/\hat{\lambda}_1^4)\{\hat{\phi}_1\} \tag{46}$$

and

$$\left[[\lambda_2^{(\ell)}[K_1] + [K_0]]^{-1}[M] - (1/\hat{\lambda}_1^4)\{\hat{\phi}_1\}\{\hat{\phi}_1\}^T[M]\right]\{\phi_2\}^{(\ell+1)} = -(1/\lambda_2^{4(\ell+1)})\{\phi_2\}^{(\ell+1)} \tag{47}$$

These relationships are used to calculate successive estimates of the second eigenvalues λ_2, again using several applications of the matrix iteration process. An initial estimate of the second eigenvalue, $\lambda_2^{(1)}$, is made and used in Eq. (46) to determine, through iteration, values of the first quasi-mode shape, $\{\hat{\phi}_1\}$, and the first quasi-eigenvalue, $\hat{\lambda}_1^4$. The values of $\{\hat{\phi}_1\}$, $\hat{\lambda}_1^4$, and $\lambda_2^{(1)}$ are then substituted into Eq. (47). The quasi-eigenvalue and -eigenvector are held fixed, and iteration is applied until the mode shape $\{\phi_2^{(1)}\}$ converges. This establishes the four values of the second estimate of the second eigenvalue, $\lambda_2^{(2)}$, and the corresponding modes shapes. Each of the second estimates of the second eigenvalue $\lambda_2^{(2)}$ are then substituted into Eq. (46) and used to improve the values of the quasi-eigenvalues and -eigenvectors. Equation (47) is then used to find new eigenvalues $\lambda_2^{(3)}$, and the entire process is repeated until convergence is achieved.

Application of Turner's method to the determination of the third eigenvalue and mode shape produces recursive relationships of the form

$$\left[\lambda_3^{(\ell)}[K_1]+[K_0]\right]^{-1}[M]\{\hat{\phi}_1\}=(1/\hat{\lambda}_1^4)\{\hat{\phi}_1\} \tag{48}$$

$$\left[[\lambda_3^{(\ell)}[K_1]+[K_0]]^{-1}[M]-\frac{1}{\hat{\lambda}_1^4}\{\hat{\phi}_1\}\{\hat{\phi}_1\}^T[M]\right]\{\hat{\phi}_2\}=-\frac{1}{\hat{\lambda}_2^4}\{\hat{\phi}_2\} \tag{49}$$

$$\left[[\lambda_3^{(\ell)}[K_1]+[K_0]]^{-1}-\frac{1}{\hat{\lambda}_1^4}\{\hat{\phi}_1\}\{\hat{\phi}_1\}^T-\frac{1}{\hat{\lambda}_2^4}\{\hat{\phi}_2\}\{\hat{\phi}_2\}^T\right][M]\{\phi_3\}^{(\ell+1)}=-\frac{1}{\lambda_3^{4(\ell+1)}}\{\phi_3\}^{(\ell+1)} \tag{50}$$

Substituting the initial estimate of λ_3 into all three equations, Eq. (48) produces $\hat{\lambda}_1$ and $\{\hat{\phi}_1\}$, Eq. (49) generates $\hat{\lambda}_2$ and $\{\hat{\phi}_2\}$, and Eq. (50) yields the next estimates of λ_3. It is to be remembered that the process is to be used for each of the branches of the fourth root of λ_3^4. The algorithm for the fourth and higher eigenvalues is evident. This numerical procedure does in fact converge to those terms appearing in the solution of Eq. (38). Unfortunately, the algorithm is not very efficient. Convergence times increase dramatically as the level of damping increases.

Having found the eigenvalues and mode shapes, we can now construct the orthogonal transformation that decouples the expanded equations of motion for forced motion [Eq. (37)]. The expanded eigenvectors appearing in Eq. (38) are constructed from the known eigenvalues λ_j and the known mode shapes $\{\phi_j\}$. The orthogonal transformation matrix $[\tilde{\phi}]$ is constructed from the expanded eigenvectors. Applying the orthogonal transformation to the equations of forced motion [Eq. (37)] produces

$$s^{1/2}[\tilde{\phi}]^T[\tilde{M}][\tilde{\phi}]\{\tilde{A}_n(s)\}+[\tilde{\phi}]^T[\tilde{K}][\tilde{\phi}]\{\tilde{A}_n(s)\}=[\tilde{\phi}]^T\{\tilde{F}(s)\} \tag{51}$$

Performing the matrix multiplications and solving for $\tilde{A}_n(s)$, the transform of the expanded modal participation factors, results in

$$\tilde{A}_n(s)=\frac{\{\tilde{\phi}_n\}^T\{\tilde{F}(s)\}}{\tilde{m}_n(s^{1/2}-\lambda_n)} \tag{52}$$

where

$$\lambda_n=-(\tilde{k}_n/\tilde{m}_n) \tag{53}$$

By virtue of the nature of the right-hand side of Eq. (37), this reduces to

$$A_n(s)=\frac{\{\phi_n\}^T\{F(s)\}}{\tilde{m}_n(s^{1/2}-\lambda_n)} \tag{54}$$

The general form of the transform of the transient response of the beam is

$$\{X(s)\}=\sum_n A_n(s)\{\phi_n\} \tag{55}$$

For a vertical unit step load at the jth DOF, this leads to

$$\{X(s)\}=\sum_n\frac{\phi_{n_j}}{\tilde{m}_n(s^{1/2}-\lambda_n)s}\{\phi_n\} \tag{56}$$

This completes the solution for the transform of the transient response as obtained by a finite element model of the beam.

Continuum Model vs Finite Element Model

To compare the results produced by the two models of the beam, we would like to determine the inverse of the transforms already found and compare the results in the time domain. However, the finite element model predicts types of motion not described by the continuum model. The continuum model is predicated on bending and axial motions only in the beam and constraining layer, respectively, and shear motion only in the constrained layer. The finite element model is not so restricted. For instance, the finite element model describes motion of the constraining layer oscillating vertically with respect to the beam, including a thickness stretch motion in the viscoelastic layer. Several motions that involve very little beam bending begin to appear at frequencies just above the second bending mode of the beam. These motions are not predicted by the continuum model because of the simplifying assumptions incorporated in its development. Consequently, the comparison of the continuum model and the finite element model will be made only in terms of motions common to both.

The time domain responses of the first two symmetric bending modes are shown in Figs. 4-7. Figures 4 and 5 are the modal participation time histories of the first two symmetric modes as predicted by the continuum model. Figures 6 and 7 are the corresponding responses from the finite element model. In both cases, the downward unit step load causing the motion is applied at midspan. In the finite element model, the unit step was applied at the center node on the horizontal midplane of the beam. The responses shown do not include the nonoscillatory motion discussed earlier.

In both cases, the transient responses have been calculated from the transforms of the transient motion using contour integration in the complex s plane and the residue theorem. The particular method used has been reported elsewhere[7] and will not be repeated here. The responses shown in Figs. 4-7 are those parts of the total response produced by the residue of the poles contributing to the contour integration process. They are the exponentially decaying sinusoidal motion about the static deflection caused by the unit step load. The viscoelastic creep behavior in the structure is accounted for by two segments of the contour integration along the branch cut of the function $s^{1/2}$. These contributions to the response are not shown in Figs. 4-7 because we wish to focus on the decaying, oscillatory bending behavior.

The responses of the first and third modes of the continuum model (Figs. 4 and 5) are calculated by taking the transform of the modal response and calculating the residues of the poles in the integrand of the inverse transform. The contributions from the residues are

$$a_n(t)=\sum_j\lim_{s\to s_j}(s-s_j)A_n(s)e^{st} \tag{57}$$

where s_j are the poles. The location of the poles associated with the first mode are

$$s_{1,2}=-38.86\pm i1431.62 \tag{58}$$

$$s_3=0+i0 \tag{59}$$

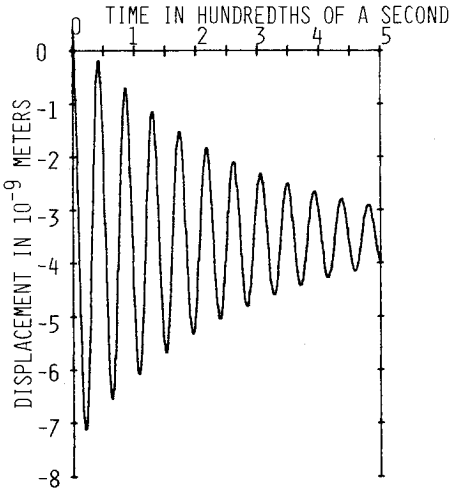

Fig. 4 First mode response for the continuum model.

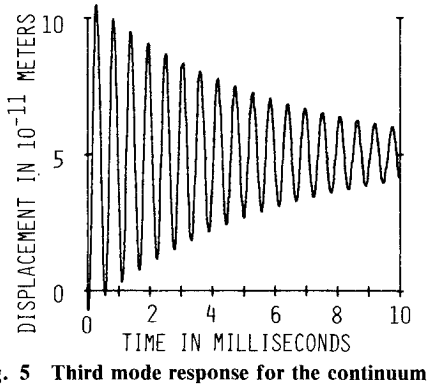

Fig. 5 Third mode response for the continuum model.

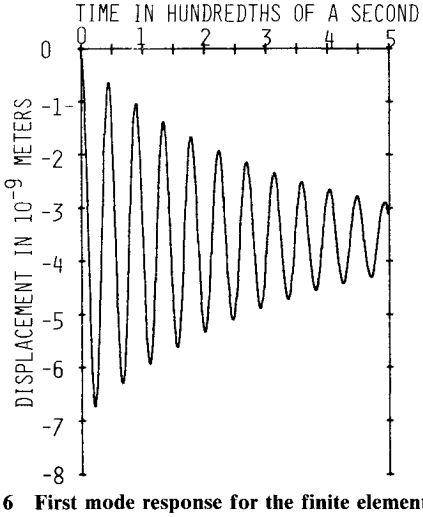

Fig. 6 First mode response for the finite element model.

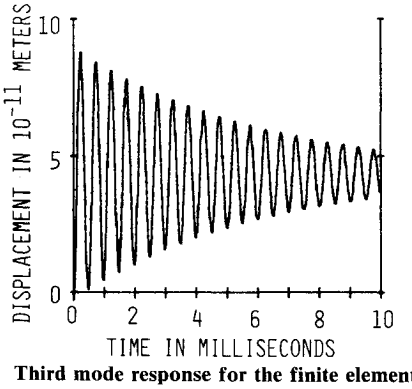

Fig. 7 Third mode response for the finite element model.

The pole at the origin describes each mode's contribution to the static deflection of the beam after the motion has died out. The poles associated with the third mode are

$$s_{1,2} = -167.48 \pm i12503.2 \tag{60}$$

$$s_3 = 0 + i0 \tag{61}$$

The responses of the first and third modes predicted by the finite element formulation (Figs. 6 and 7) are calculated in essentially the same manner. The four terms produced by Eq. (56) associated with the first mode as identified. The sum of these terms is substituted into Eq. (57) and the residues are calculated. The poles associated with the first mode shape are

$$s_{1,2} = -32.39 \pm i1402.24 \tag{62}$$

$$s_3 = 0 + i0 \tag{63}$$

The third mode response is calculated using the same method. Those poles associated with the third mode shape are

$$s_{1,2} = -177.48 \pm i11281.1 \tag{64}$$

$$s_3 = 0 + i0 \tag{65}$$

The poles and their corresponding residues are real or occur in complex conjugate pairs and the predicted structural responses are real. The modal responses are discontinuous at time zero, but these responses are not the total responses of the beam. The proof that the total response of systems such as this is continuous for all time is given elsewhere.[2] This proof also assures that the total response of the beam is always causal.

Close examination in Figs. 4-7 shows some differences between the responses predicted by the continuum and finite element formulations. The finite element formulation predicts a smaller amplitude of first mode motion and larger amplitude of third mode motion than the continuum formulation. The finite element formulation also predicts slightly lower frequencies of oscillation which decay to slightly larger static deflections than those predicted by the continuum model. These differences occur because the continuum model is based on a Euler beam, which does not allow shear strain in the beam, whereas the finite element model uses quadratic strain triangles in the beam, and these elements do allow shear strain. In light of this, it is to be expected that the finite element formulation predicts a more flexible beam.

Conclusions

The fractional calculus model was incorporated without difficulty into the standard continuum model of the beam with a constrained layer damping addition. For simple structures such as this, it has been demonstrated that transient responses may be computed while using a material model that describes well the behavior of viscoelastic materials over a wide range of frequencies. The superior material model enables results to be obtained more accurately and efficiently than otherwise possible.

However, not all structures may be modeled with a simple continuum formulation such as that employed here. In many cases, the finite element method has great utility. It has been shown here that the desirable features of the fractional calculus model may be retained while employing a finite element solution for the transient motion of viscoelastically damped structures. The satisfactory agreement between the results obtained through continuum and finite element formulations confirms the effectiveness of the special numerical methods developed for the solution of the matrix equations.

Acknowledgments

This work was sponsored by the Metals Behavior Branch of the Materials Laboratory, Wright Aeronautical Laboratories,

Wright-Patterson AFB, Ohio. In particular, we are indebted to Drs. Jack Henderson, David Jones, Ted Nicholas, and Lynn Rodgers of the Wright Aeronautical Laboratories for their continued interest and support. We are also indebted to Master Sergeant John Ullum, who did the artwork, and to Ms. Amy Moore for the preparation of the manuscript.

References

[1]Bagley, R. L. and Torvik, P. J., "A Theoretical Basis for the Application of Fractional Calculus to Viscoelasticity," *Journal of Rheology*, Vol. 27, June 1983, pp. 201-210.

[2]Bagley, R. L., *Applications of Generalized Derivatives to Viscoelasticity*, Ph.D. Dissertation, Air Force Institute of Technology; also published as Air Force Materials Laboratory TR-79-4103, Nov. 1979.

[3]Bagley, R. L. and Torvik, P. J., "A Generalized Derivative Model for an Elastomer Damper," *The Shock and Vibration Bulletin*, No. 49, Pt. 2, Sept. 1979, pp. 135-143.

[4]Bagley, R. L., "Fractional Derivative Models for a Family of Corning Glasses, AFWL technical report, to be published.

[5]Bagley, R. L., "Fractional Derivative Models for a Family of Assorted Glassy Enamels," AFWL technical report, to be published.

[6]Bagley, R. L., "Fractional Derivative Models for Assorted Polymers," AFWL technical report, to be published.

[7]Bagley, R. L. and Torvik, P. J., "Fractional Calculus—A Different Approach to the Analysis of Viscoelastically Damped Structures," *AIAA Journal*, Vol. 21, May 1983, pp. 741-748.

[8]Rogers, L., "On Modeling Viscoelastic Behavior," *The Shock and Vibration Bulletin*, No. 51, 1981, pp. 55-69.

[9]Gross, B., "On Creep and Relaxation II," *Journal of Applied Physics*, Vol. 19, March 1948, pp. 257-264.

[10]Crandall, S. H., "Dynamic Response of Systems with Structural Damping," *Air, Space and Instruments, Draper Anniversary Volume*, edited by H. S. Lee, McGraw-Hill Book Co., New York, 1963, pp. 183-193.

[11]Nutting, P. G., "A New Generalized Law of Deformation," *Journal of the Franklin Institute*, Vol. 191, 1921, pp. 679-685.

[12]Graham, A., "The Phenomenological Method of Rheology," *Research*, Vol. 6, London, 1953, pp. 92-96.

[13]Caputo, M., *Elasticita e Dissipazione*, Zanichelli, Bologna, 1969.

[14]Slonimsky, G. L., "Laws of Mechanical Relaxation Process in Polymers," *Journal of Polymer Science*, Pt. C, No. 16, 1967, pp. 1667-1672.

[15]Smit, W. and deVries, H., "Rheological Models Containing Fractional Derivatives," *Rheologica Acta*, Vol. 9, 1970, pp. 525-534.

[16]Calleja, R. D. and Guzman, G. M., "Application of the Method of Fractional Derivatives to Obtain Time Relaxation Spectra From Viscoelastic Dynamic Data," *Anales de Fisica de la Read Sociedad Espanola de Fisica y Quimica*, Vol. 71, Oct.-Dec. 1975, pp. 277-279.

[17]Shestopal, V. O., "Diffusion of Vacancies and High Temperature Rheological Properties of Metals," *Fizika Tverdogo Tela*, Vol. 12, No. 1, 1970, pp. 291-293.

[18]Shermergor, T. D., "On the Use of Fractional Differentiation Operators for the Description of Elastic Aftereffect Properties of Materials," *Zhurnal Prikladnoi Mekhaniki i Teknicheskoi Fiziki*, Vol. 7, No. 6, 1966, pp. 118-121 (pp. 85-87 in trans).

[19]Torvik, P. J. and Bagley, R. L., "On the Appearance of the Fractional Derivative in the Behavior of Real Materials," *Journal of Applied Mechanics*, Vol. 51, June 1984, pp. 294-298.

[20]Ross, B., "A Brief History and Exposition of the Fundamental Theory of Fractional Calculus," *Lecture Notes in Mathematics*, Vol. 457, Springer-Verlag, New York, 1975, pp. 1-36.

[21]Madegowsky, W. M., private communication, Naval Surface Weapons Center, White Oak, Silver Spring, Md.

[22]Roberts, D. J. and Madegowsky, W. M., *Dynamic Viscoelastic Properties of Materials, Part III*, Naval Surface Weapons Center, Silver Springs, Md., TR-80-425, Sept. 1980.

[23]Rouse, P. E. Jr., "The Theory of the Linear Viscoelastic Properties of Dilute Solutions of Coiling Polymers," *The Journal of Chemical Physics*, Vol. 21, No. 7, 1953, pp. 1272-1280.

[24]Ferry, J. D., Landel, R. F., and Williams, M. L., "Extensions of the Rouse Theory of Viscoelastic Properties to Undiluted Linear Polymers," *Journal of Applied Physics*, Vol. 26, No. 4, 1955, pp. 359-362.

[25]DiTaranto, R. A., "Theory of Vibratory Bending for Elastic and Viscoelastic Layered Finite-Length Beams," *Journal of Applied Mechanics*, Vol. 32, Dec. 1965, pp. 881-886.

[26]Torvik, P. J., "The Analysis and Design of Constrained Layer Damping Treatments," *Damping Applications for Vibration Control*, ASME, New York, 1980, pp. 85-112.

[27]Mead, D. J. and Markus, S., "The Forced Vibration of a Three Layered Damped Sandwich Beam with Arbitrary Boundary Conditions," *Journal of Sound and Vibration*, Vol. 10, No. 2, 1969, pp. 163-175.

[28]Christensen, R. M., *Theory of Viscoelasticity, An Introduction*, Academic Press, New York, 1971, pp. 207-218.

[29]Cook, R. D., *Concepts and Applications of Finite Element Analysis*, 2nd Ed., John Wiley, New York, 1981, pp. 191-195.

[30]Bisplinghoff, R. L., Ashley, H., Halfman, R. L., *Aeroelasticity*, Addison-Wesley, Reading, Mass., 1955, p. 168.